

[Click here to view linked References](#)

1 **The Variscan basement in the western shoulder of the Lusitanian Basin**
2 **(West Iberian Margin). Insights from detrital-zircon geochronology of**
3 **Jurassic strata**

4
5
6
7 5 Pedro A. Dinis ¹, Pieter Vermeesch ², Luís V. Duarte ¹, Pedro P. Cunha ¹, Marta
8 6 Barbarano ³, Eduardo Garzanti ³

9
10
11
12 8 ¹ University of Coimbra, Marine and Environmental Sciences Centre (MARE), Department
13 9 of Earth Sciences, Rua Sílvio Lima, 3030-790 Coimbra, Portugal

14
15 10 ² London Geochronology Centre, Department of Earth Sciences, University College
16 11 London, London WC1E 6BT, UK

17
18 12 ³ Laboratory for Provenance Studies, Department of Earth and Environmental Sciences,
19 13 University of Milano-Bicocca, 20126 Milano, Italy

20
21
22 14
23 15 **Abstract:** There is no consensus about the geological nature of the westernmost portion
24 16 of the Iberian Massif. In the present research, the detrital zircon U-Pb signatures of
25 17 Jurassic strata of the Lusitanian Basin, known to be west-sourced, are combined with
26 18 published U-Pb data for the Precambrian-Palaeozoic basement and the Lusitanian Basin
27 19 units to better understand this poorly exposed portion of the Iberian Massif. Cryogenian to
28 20 Ediacaran ages prevail in a northern Upper Jurassic unit, while Lower and Upper Jurassic
29 21 rocks in southern locations yield mostly Carboniferous to upper Permian zircons. These
30 22 age results, coupled with their respective U/Th ratios, suggest that the basin covers two
31 23 distinct terranes of the Iberian Massif. Another noteworthy feature of west-derived
32 24 deposits is the abundance of <310 Ma ages. It is proposed that a combination of crustal
33 25 thinning in the West Iberian Margin with regional eastward basement tilt, favoured the
34 26 enrichment of relatively young zircon in the western shoulder of the basin relative to its
35 27 eastern margin. The detrital zircon age signatures also reveal a middle to late Permian
36 28 thermal event in restricted areas, which is probably associated with the oldest stages of
37 29 Alpine extension in West Iberia.

38
39 30
40 31 **Keywords:** Detrital zircon geochronology, Provenance, Jurassic, Berlengas Block, West
41 32 Iberian Margin

42 33

1 Introduction

Three major tectono-stratigraphic units with Gondwana affinity (Galicia — Trás-os-Montes Zone, GTMZ), Central Iberian Zone, CIZ) and Ossa Morena Zone, OMZ) and one unit with Avalonian affinity (South Portuguese Zone, SPZ) crop out in the western portion of the Iberian Massif (e.g., Quesada 1991, Simancas et al. 2019). The rocks that are exposed to the west of the Porto-Tomar Fault Zone (PTFZ), both in the Iberian mainland and in the Berlengas Archipelago, have been assigned to different geotectonic units. Classic perspectives consider that they are part of the OMZ (Julivert et al. 1974; Ribeiro et al. 1990; Oliveira et al. 1992). Recently, however, it was proposed that the PTFZ separates the autochthonous or parautochthonous units of the CIZ and OMZ from a western crustal block called Finisterra Terrane, which includes the Berlengas Archipelago (Ribeiro et al. 2007; Moreira et al. 2019). Others proposed a simplification by merging the OMZ and GTMZ in a single unit and assigning the region to the west of the PTFZ to the SPZ (Díez-Fernández and Arenas 2015, Arenas et al. 2016, Díez Fernández et al. 2016). Tectonic models for the Variscan-Alleghanian orogen necessarily depend on possible stratigraphic assignments for the westernmost part of the Iberian Massif.

Sediment composition provides a broad picture of basement units that were exposed at the time of formation of depositional sequences, complementing what can be acquired from the direct investigation of possible source-rock units. Where basement exposures are scarce or difficult to access, sedimentary deposits can offer the best way to investigate the geological nature of regional crustal blocks. In addition, the infill of a sedimentary basin is likely able to reveal a history of exhumation, including rock units placed in upper crustal levels that are no longer available for direct investigation (Dickinson 1985, Garzanti 2016). Detrital zircon-age signatures prove to be an excellent tool when attempting to reconstruct the exhumation history of orogenic chains (e.g., Bernet et al. 2006, Gehrels 2014, Wang et al. 2016). Despite the uncertainties regarding zircon productivities, which necessarily depend on source rock composition (Rino et al.

62 2004, Moecher and Samson 2006, Hawkesworth et al. 2013), and the climatic and
63 orographic setting that, by influencing clastic supply, also affect age signatures (Malusà
64 and Garzanti 2019), the detrital zircon record of sedimentary units helps to understand the
65 geological nature of their source terranes.

66 It has been considered that the Berlengas Block was the source area for several Lower to
67 Upper Jurassic formations exposed onshore of the westernmost sector of the Lusitanian
68 Basin (e.g., Wright and Wilson 1984, Guéry et al. 1986, Wilson 1989, Duarte 1997, Pena
69 dos Reis et al. 1996, 2000, Ravnås et al. 1997, Barata et al. 2021). The present
70 investigation is focused on the detrital-zircon age signature of a selection of Jurassic units
71 enriched in siliciclastic components with that provenance. These geochronological data
72 provide precious information about the basement rocks exposed at the time of the
73 Lusitanian Basin infill. The geology of the western part of the Iberian Massif is crucial for
74 the understanding of the evolution of West Europe and its conjugate margin in North
75 America since the time of Pangea amalgamation.

76

77 **2 The Lusitanian Basin**

78 2.1 Tectonic framework

79 During the Triassic to Jurassic, the Lusitanian Basin (LB) overlies the Iberian Massif
80 between the PTFZ, to the east, and the Berlengas Block, to the west (Fig. 1). The western
81 part of the Iberian Massif comprises a series of upper Neoproterozoic to Paleozoic
82 metasedimentary successions along with magmatic rocks and metamorphic units with
83 igneous protolith, including pre-Variscan (mainly upper Ediacaran and Cambrian-lower
84 Ordovician) and Variscan to post-Variscan (i.e., Upper Devonian–Permian) (e.g., Oliveira
85 et al. 1992, Simancas 2019). Depending on regional models for the tectono-stratigraphy of
86 the Iberian Massif, the Triassic and Jurassic infill of the LB stands either on the OMZ
87 (Oliveira et al. 1992), the Finisterra Terrane (Ribeiro et al. 2007, Moreira et al. 2019), or

88 units akin to the Avalonia terrane, including the SPZ (Simancas et al. 2005, Díez
1
2 89 Fernández and Arenas 2015, Arenas et al. 2016, Díez Fernández et al. 2016).
3
4
5 90 The Berlengas Archipelago (Fig. 1), with the Berlengas and Farilhões groups and the
6
7 91 Estelas islets, is the westernmost outlier of the Iberian Massif (Freire de Andrade 1937,
8
9 92 Vanney and Mougénou 1981). It is a horst block (hereafter referred to as the Berlengas
10
11 93 Block) separating the LB from an external domain of the West Iberian Margin that includes
12
13 94 the Peniche Basin (e.g., Alves et al. 2006, Terrinha et al. 2019). The archipelago's rocks
14
15 95 include granites in Berlenga and Estelas, and migmatites, gneisses and micaschists in
16
17 96 Farilhões. A few geochronological studies have been presented for the archipelago. The
18
19 97 Berlengas granite yields zircon and monazite dated by ID-TIMS at 305.2 Ma (Valverde
20
21 98 Vaquero et al. 2011). However, previous studies, based on $^{87}\text{Rb}/^{86}\text{Sr}$ data for whole rock,
22
23 99 pointed to a younger Permian age (280 ± 15 Ma; Priem et al. 1965). Monazite retrieved
24
25 100 from a two-mica granite of Farilhões provided a concordia age of 376 ± 3 Ma (Valverde
26
27 101 Vaquero et al. 2011).
28
29
30
31 102 After the Variscan cycle, which completed the assemblage of the Iberian Massif, an
32
33 103 extensional phase, related to final Variscan orogenic collapse, started during the early
34
35 104 Permian in eastern and central Iberia (e.g., Arche and López-Gómez 1996, Arche et al,
36
37 105 2004, López-Gómez et al. 2019, 2021). In western Iberia, the oldest units related to
38
39 106 Pangea break-up are dated as Triassic (Palain 1976, Pinheiro et al. 1996, Soares et al.
40
41 107 2012). Mesozoic rifting climaxed during the Oxfordian (Late Jurassic) (Wilson et al. 1989,
42
43 108 Pena dos Reis et al. 1996, 2000, Leinfelder and Wilson 1998, Alves et al. 2002, 2006,
44
45 109 Pereira et al. 2017) and was associated with the formation of N-S trending extensional
46
47 110 basins, namely the Lusitanian and Peniche basins at mid latitudes of west Iberia (Alves et
48
49 111 al. 2006, Terrinha et al. 2019). It is usually considered that the Mesozoic evolution of the
50
51 112 west Iberia margin was controlled by four main tectono-stratigraphic phases (Wilson et al.
52
53 113 1989): (1) Middle(?)/Late Triassic to Callovian; (2) middle Oxfordian to Berriasian; (3) late
54
55 114 Berriasian to late Aptian; (4) late Aptian to early Campanian. During the Triassic, the
56
57 115 eastern border of the LB was controlled by the reactivation of the PTFZ (Pinheiro et al.
58
59
60
61
62
63
64
65

116 [1996](#), Soares et al. [2012](#)). The uplift of the Berlengas Block, limiting the basin to the west,
117 is indicated by west-derived clastic deposits in the uppermost Lower Jurassic succession
118 (Toarcian; e.g., Wright and Wilson [1984](#), Duarte [1997](#), Barata et al. [2021](#)), but was
119 probably also active during the Triassic. Later, the Late Jurassic rifting created several
120 sub-basins separated by crustal faults within the LB (e.g., Wilson [1979](#), Alves et al [2003b](#),
121 Taylor et al. [2014](#)), with the continental breakup between Iberia and Newfoundland being
122 achieved during the middle Aptian (Dinis et al. [2008](#), Stapel et al. [1996](#), Rasmussen et al.
123 [1998](#), Alves et al. [2002](#), [2003a](#)).

124 125 2.2 Stratigraphy

126 The LB shows a locally > 5-km-thick sedimentary infill, comprising siliciclastic and carbonate
127 units deposited in alluvial fan to hemipelagic environments and dated between the
128 Middle(?) / Upper Triassic and the Early Cretaceous, which includes at least three first-order
129 sequences bounded by regional unconformities (UBS; unconformity-bounded sequences):
130 Middle(?) / Upper Triassic-Callovian, middle Oxfordian-lower Berriasian, and Berriasian-
131 lower Aptian (e.g., Wilson et al. [1989](#), Alves et al. [2002](#), Azerêdo et al. [2003](#)). The first two
132 UBS encompass the stratigraphic intervals studied here.

133 The UBS1 starts with mainly Upper Triassic to lowermost Jurassic clastic deposits of
134 variable grain-size deposited in alluvial fan, fluvial, and lacustrine environments (Palain
135 [1976](#), Soares et al. [2012](#)). This succession is followed by Lower and Middle Jurassic
136 dolomites, carbonate-ramp marls, marly limestones and limestones, locally with significant
137 siliciclastic component (e.g., Wright and Wilson [1984](#), Duarte [1997](#), Azerêdo [1998](#), Azerêdo
138 et al. [2003](#), Duarte et al. [2012](#), Soares et al., [2012](#)). The UBS2 (middle Oxfordian to
139 lowermost Berriasian) reflects the independent evolution of sub-basins created during the
140 Late Jurassic rifting. It comprises fresh-water to brackish carbonate units at the base,
141 followed by marine carbonates and deltaic to alluvial-fan siliciclastic deposits (e.g.,
142 Leinfelder and Wilson [1998](#), Pena dos Reis et al. [1996](#), [2000](#), Rasmunssen et al. [1998](#)).

143 Most of the LB infill documents a dominant siliciclastic source from the eastern margin of
144 the LB. However, in the westernmost part of central mainland Portugal, several Jurassic
145 and Cretaceous lithostratigraphic units record a western siliciclastic supply derived from the
146 Berlengas Block. This provenance is supported by paleocurrent indicators, clast
147 composition, and interpreted paleogeography (e.g., Hill 1989, Ravnås et al. 1997, Pena dos
148 Reis et al. 2000).

149

150 **3 Materials and methods**

151 **3.1 Studied successions**

152 Three Jurassic units exposed along the western limit of the onshore LB and displaying clear
153 evidence of supply from its western shoulders were selected for the present study (Figs. 1-
154 3). This set of units provides unique conditions to indirectly assess the geological nature of
155 the Berlengas Block. Cretaceous successions with paleocurrents indicating feeding
156 systems from the west were not considered because the probability of including sediment
157 recycled from the eastern flank of the basin is expected to increase in younger deposits. On
158 the other hand, Triassic siliciclastic deposits are exposed only in the eastern basin margin,
159 where they are associated with short-distance supply from the east (Palain 1976, Soares et
160 al. 2012, Dinis et al. 2018). Samples for zircon geochronology were retrieved from the Lower
161 Jurassic Cabo Carvoeiro Formation and the Upper Jurassic Abadia and Alcobaça
162 formations.

163 The sampled Cabo Carvoeiro 2 member of Cabo Carvoeiro Fm. crops out in Praia do Abalo
164 (LJ-Ab; Figs. 1-3), where it is part of a thick carbonate succession exclusively observed in
165 the Peniche peninsula (e.g., Wright and Wilson 1984, Duarte 1997, Duarte et al. 2017,
166 Barata et al. 2021). This member is a marly-dominated unit (~ 25 m thick), well dated as
167 early Toarcian by ammonites (Duarte and Soares 2002), that includes sandy limestones,
168 feldspatho-quartzose calcareous sandstones and microconglomerates, all of them showing
169 typical turbidite features (e.g., Wright and Wilson 1984, Duarte 1997). Laterally, towards the

170 east of the basin, the Cabo Carvoeiro Formation passes to hemipelagic marl-limestone
171 alternations deposited in a carbonate ramp setting (S. Gião Fm.; Duarte 1997, Duarte and
172 Soares 2002).

173 The Alcobaça Fm. comprises marginal-marine, brackish and continental carbonates and
174 siliciclastic rocks. This unit is classically considered to span most or even all the
175 Kimmeridgian (e.g., Rasmussen et al 1998). Based on ammonite stratigraphy, Marques et
176 al. (1992) considered that it can reach the lower Tithonian, whereas Schneider et al. (2009),
177 based on Sr isotopes, proposed a latest Oxfordian to late Kimmeridgian age. A meter-thick
178 sandstone bed within a mud-dominated succession deposited in fluvio-deltaic environment
179 that is exposed in Praia da Gralha (São Martinho do Porto) was selected for detrital zircon
180 geochronology (Figs. 1-3).

181 The Abadia Fm. is considered to be a basinal lateral equivalent, to the south, of the
182 Alcobaça Fm. (Rasmussen et al 1998, Pena dos Reis et al 2000, Schneider et al 2009,
183 Kullberg and Rocha 2014). This unit comprises deep-water marls and turbiditic sandstones,
184 along with coarse-grained submarine deposits. Paleocurrent data and depositional
185 architecture of marine sandstone-conglomerates of the Abadia Fm. and transition to
186 overlying fluvial deposits of the Lourinhã Fm. are robust evidence of provenance from the
187 west (Ellwood 1987, Hill 1989, Ravnås et al. 1997). A 3 m thick sandstone bed from the
188 upper part of Abadia Fm. exposed in Praia da Amoreira beach was selected for this study
189 (Figs. 1-3). These deposits belong to a succession of steeply inclined sandstone
190 intercalated with heterolithic beds interpreted as either foreset-bottomset units of a
191 prograding fan delta (Ravnås et al. 1997) or as the infill of a submarine channel (Ellwood
192 1987).

193

194 3. Analytical and statistical procedures

195 Separation of zircon grains was carried out at the Earth Sciences Department of University
196 of Coimbra. Samples were manually disintegrated, and the fractions finer than 0.038 mm

197 and coarser than 0.5 mm were removed through wet sieving. Heavy liquids (sodium
198 polytungstate and methylene iodide) and a Frantz isodynamic magnetic separator were
199 used to obtain the zircon concentrates. An aliquot of heavy-mineral concentrates before the
200 magnetic separation was mounted on glass slides and analyzed under the petrographic
201 microscope. U-Pb ages were determined at the London Geochronology Centre using an
202 Agilent 7700× LA-ICP-MS (laser ablation-inductively coupled plasma-mass spectrometry)
203 system, employing a NWR193 Excimer Laser operated at 11 Hz with a 20 µm spot size and
204 2.5–3.0 J/cm² fluence.

205 Data reduction was performed using GLITTER 4.4.2 software (Griffin et al. 2008). We used
206 ²⁰⁶Pb/²³⁸U and ²⁰⁷Pb/²⁰⁶Pb ages for zircons younger and older than 1100 Ma, respectively.
207 No common Pb correction was applied. The original data was screened through these
208 discordance filters and grains with >5–15% age discordances were discarded. Data was
209 plotted as Kernel density estimations with different bandwidths using *DensityPlotter*
210 software (Vermeesch 2012). Multidimensional Scaling (MDS) was adopted to compare the
211 obtained age results with possible source terranes. MDS is a multivariate technique that
212 takes a dissimilarity matrix as input to obtain a map where similar samples plot close
213 together and dissimilar samples plot far apart. To perform the MDS with detrital zircon age
214 distribution, a dissimilarity matrix was constructed using the Kolmogorov-Smirnov statistic
215 (Vermeesch 2013).

216

217 **4 Results**

218 *4.1 Heavy minerals*

219 Heavy-mineral concentrates obtained from the lower Toarcian turbidite of the Cabo
220 Carvoeiro Fm. (LJ-Ab) include abundant chlorite and significant amounts of rock fragments
221 and light minerals. The translucent heavy mineral assemblage yields mainly the durable
222 minerals zircon and tourmaline. The Kimmeridgian beds provided substantially different

223 heavy-mineral assemblages. In the northern sample from the Alcobaça Fm., staurolite,
224 garnet and dravitic tourmaline dominate the assemblage. The southern sample (from the
225 Abadia Fm.) yielded zircon and subordinate tourmaline, garnet, and monazite.

226

227 *4.2 Detrital zircon U-Pb data*

228 Samples LJ-Ab (lower Toarcian, Cabo Carvoeiro Fm.) and UJ-Am (Kimmeridgian, Abadia
229 Fm.) yielded similar zircon-age signatures (Fig. 4). The zircon grains are mainly
230 Carboniferous-Permian (85%, ranging 349-254 Ma, in LJ-Ab; 80%, ranging 339-276 Ma, in
231 UJ-Am). The KDE spectrum for the Toarcian sample (LJ-Ab) reveals two peak maxima at
232 approximately 305 Ma and 292 Ma and a secondary peak at 264 Ma; the Kimmeridgian-
233 Tithonian sample (UJ-Am) yields a sharp peak at 295 Ma. Cryogenian to Ediacaran zircons,
234 ranging in age 692-556 Ma, occur in secondary amounts (17% in LJ-Ab; 13 % in UJ-Am)
235 and both samples gave one Middle Triassic grain (243 Ma in LJ-Ab; 230 Ma in UJ-Am).

236 The Kimmeridgian bed from Alcobaça Fm. (UJ-Gr) is dominated by Cryogenian to
237 Ediacaran grains (83 % ranging 673-543 Ma), with frequency peaks at 608, 595, 580, and
238 554 Ma (Fig. 4). Cambrian-Silurian (7%, ranging 541-456 Ma), Paleoproterozoic (3%,
239 ranging 541-456 Ma Ma) and Carboniferous-Permian (342 Ma and 273 Ma) grains are
240 subordinate to minor.

241 Th/U ratios obtained during laser ablation range 0.05 - 1.15 (Fig. 5). Cryogenian-Ediacaran
242 zircons tend to yield higher Th/U than Carboniferous-Permian grains. Th/U ratios for the
243 majority of grains of this age retrieved from UJ-Am (Kimmeridgian, Abadia Fm.) are
244 relatively low, whereas those from LJ-Ab (Toarcian, Carbo Carvoeiro Fm.) are more
245 variable.

246

247

249 **5 Discussion**

250 5.1. Zircon sources and corresponding terranes

251 The late Cryogenian-Ediacaran population, well represented in UJ-Gr and prevalent in
252 many Mesozoic units of West Iberia (Dinis et al. 2016, 2018, Pereira et al. 2016, 2017), is
253 also dominant in most basement units of West Iberia (Linnemann et al. 2008, Talavera et
254 al. 2012, Pereira et al. 2012a, 2012b, 2014, Rodrigues et al. 2015). These ages correspond
255 with the Pan-African to Cadomian orogenies, two periods of crustal growth that overlap in
256 northern Gondwana realms (Murphy and Nance 1991, Nance and Murphy 1994, Linnemann
257 et al. 2008).

258 The oldest peak within the Carboniferous-Permian age population (~315 Ma in UJ-Am;
259 ~305 Ma in LJ-Ab) corresponds to the paroxysmal stages of Variscan collisional magmatism
260 in Iberia, which started at ~350 Ma and persisted for almost the entire Carboniferous (Dias
261 et al. 1998, Fernández-Suárez et al. 2000, Jesus et al. 2007, Hildenbrand et al. 2021).
262 Magmatic rocks of this age are also well represented in the conjugate West Atlantic margin
263 in the easternmost terranes of the Appalachian Orogen (MacLean et al. 2003, Pe-Piper et
264 al. 2010). Zircon grains potentially derived from those primary sources are common in
265 Mesozoic units of the West Iberian Margin (Dinis et al. 2016, 2018, Pereira et al. 2016,
266 2017) and of its Canadian conjugate margin (Lowe et al. 2011, Hutter and Beranek 2020).
267 The ~290-295 Ma peaks identified in southern samples (LJ-Ab and UJ-Am) are genetically
268 linked to post-Variscan magmatism coeval to the post-orogenic collapse of the Variscan
269 chain (Marques et al. 2002, López-Gómez et al. 2019, 2021, Hildenbrand et al. 2021) or the
270 buckling of the Cantabrian orocline (Gutiérrez-Alonso et al. 2004, 2011, Merino-Tomé et al.
271 2009, Pastor-Galán et al. 2013). Similar zircon ages are common in some Cretaceous
272 strata of the West Iberian Margin (Dinis et al. 2016) and occur in the Permian Viar Basin
273 formed ~350 km SE-ward, where they were either exhumed from high crustal levels or
274 extruded during volcanic events (Dinis et al. 2018).

1
2
3
4
5
6
7
8
9
10
11
12
13
14
15
16
17
18
19
20
21
22
23
24
25
26
27
28
29
30
31
32
33
34
35
36
37
38
39
40
41
42
43
44
45
46
47
48
49
50
51
52
53
54
55
56
57
58
59
60
61
62
63
64
65

275 The secondary middle Permian peak at ~264 Ma (exclusive of LJ-Ab) is notably younger
276 than the main phases of Pangea amalgamation. These zircons, along with the rare Middle
277 Triassic grains, are probably associated with subsequent Pangea break-up in West Iberia.
278 Grains of comparable age were identified in Triassic (Dinis et al. 2018) and Cretaceous
279 (Dinis et al. 2016) lithostratigraphic units of the LB, being ascribed to mafic magmatism
280 during early stages of extension (Gardien and Paquette 2004, Orejana et al. 2008).

281 To better link the obtained age distributions with possible source terranes, an MDS was
282 performed. Taking as input the entire dataset obtained for the three Jurassic units and age
283 results published elsewhere for west Iberia basement units, the MDS map separates LJ-Ab
284 (lower Toarcian, Cabo Carvoeiro Fm.) and UJ-Am (Kimmeridgian, Abadia Fm.) from all
285 basement units, and plots UJ-Gr (Kimmeridgian, Alcobaça Fm.) close to OMZ and CIZ (Fig.
286 6). The field for SPZ is wider, reflecting high compositional variability mainly determined by
287 the proportion of Variscan grains, which are abundant in some units but rare or absent in
288 others (Pereira et al. 2012b, 2014, Rodrigues et al. 2015). The isolated location of LJ-Ab
289 and UJ-Am in the MDS map is explained by their enrichment in relatively young grains.

290 The variability in zircon age distributions for each major tectono-stratigraphic unit of the
291 Iberian basement and the similarities among them do not allow conclusive interpretations
292 regarding the basement of the LB. The zircon age signatures, however, do not indicate that
293 they belong to a Finisterra Terrane (Ribeiro et al. 2007, Moreira et al. 2019). The west-
294 derived deposits of the LB lack zircon ages that occur in metamorphic units ascribed to the
295 Finisterra terrane, such as Ordovician (Sousa et al. 2014, Moreira et al. 2019) and Upper
296 Silurian-Early Devonian and Early Devonian-Mississippian (Almeida et al. 2014). These
297 ages are represented in sedimentary successions formed close to the PTFZ (Dinis et al.
298 2012, 2018), along which most rock units assigned to the Finisterra Terrane are presently
299 exposed. Mesoproterozoic zircons in the Pennsylvanian Buçaco Basin were also
300 considered to be derived from the Finisterra Terrane (Moreira et al. 2019), but these ages
301 are also missing in west-derived deposits of the LB. It can be alleged that, as the above-

302 mentioned age populations are not abundant in sedimentary deposits formed close to the
303 PTFZ, the presence of a clearly dominant younger population in LJ-Ab and UJ-Am probably
304 diluted the detrital fingerprint, making those ages common in Finisterra Terran harder to
305 identify. However, they are also missing in UJ-Gr, which lacks the young age population.

306

307 5.2. Tectono-stratigraphic implications

308 At the latitude of Peniche and to the south, Variscan igneous rocks must have been
309 extensively exposed in the western flank of the LB during the Jurassic stages of Pangea
310 break-up. To the north, instead, they appear to be minor zircon suppliers. The different age
311 signature in northern locations is ascribed to a scarcity of Variscan magmatic outliers or to
312 dilution by other zircon sources. The heavy-mineral assemblage characterized by dominant
313 garnet and staurolite supports a high-grade metamorphic provenance. Part of the Pan-
314 African to Cadomian-aged zircons may be recycled from Triassic units deposited during the
315 early stage of Pangea break-up, where this age population is frequently the most abundant
316 (Pereira et al. [2016](#), [2017](#), Dinis et al. [2018](#)).

317 A dyke-breccia in Peniche, close to the studied Cabo Carvoeiro Fm. at Praia do Abalo,
318 includes granitic xenoliths that yield late Pennsylvanian-early Permian zircons (Pereira et
319 al. [2020](#)), suggesting that the LB developed on a crustal block with late and post-Variscan
320 magmatic rocks. In the LB, the frequency of <310 Ma-aged zircons is a noteworthy feature
321 of the signature of the studied west-derived strata. The late Paleozoic population identified
322 in Triassic units of the Algarve and Alentejo basins, which were mainly sourced from the
323 SPZ, is notably older (~330 Ma; Pereira et al. [2016](#); Dinis et al. [2018](#)). Some Triassic rocks
324 overlying the OMZ yield an only minor frequency peak <300 Ma (Dinis et al. [2018](#)). For
325 Cretaceous successions of the LB, late Paleozoic peaks tend to become younger upward,
326 possibly due to the exhumation of progressively younger igneous rocks emplaced in the
327 uplifted CIZ, but the maxima for Lower Cretaceous units are in general >300 Ma (Dinis et
328 al. [2016](#)). Only in stratigraphic units approximately 40 Ma younger than the youngest west-

329 derived units presented here the late Paleozoic populations display major peaks at ~295-
1
2 330 290 Ma.
3
4

5 331 In summary, in the LB, the late Paleozoic zircon-age population appears to be younger in
6
7 332 successions mainly sourced from the west than in those sourced from the east. Such an
8
9 333 age difference probably results from more extensive crustal thinning in the western margin
10
11 334 than for inland Iberian regions, allowing for the emplacement of igneous rocks into upper-
12
13 335 crustal levels. The Berlengas Block is presently placed in a necking sector between hyper-
14
15 336 thinned and proximal realms of crustal margin (Stanton et al. 2016, Granado et al. 2021),
16
17 337 but significant thinning would be necessary by early Permian. The 295-285 Ma interval was
18
19 338 already proposed to be characterized by post-orogenic extension (Variscan orogenic
20
21 339 collapse) in West Iberia and associated with the uplift of the CIZ relative to OMZ
22
23 340 (Hildenbrand et al 2021). Additionally, a rapid exhumation of recently formed primary zircon
24
25 341 sources in the western shoulder of the basin may have been triggered by the eastward
26
27 342 tilting of the basin basement (Fig. 7). The geometry of the basement top, as recognized in
28
29 343 several seismic lines (e.g., Alves et al 2006, Pereira et al 2017), is compatible with this
30
31 344 possibility.
32
33
34
35

36
37 345 Further inferences can be drawn from Th/U ratios. Although this parameter even for single
38
39 346 magmatic bodies can be widely variable, it has been used to assess temperatures of zircon
40
41 347 crystallization and the felsic vs. intermediate character of the host rocks. Under equilibrium
42
43 348 conditions, Th/U ratios tend to be higher in zircons formed at higher temperatures and in
44
45 349 intermediate/mafic rocks than at lower temperatures and in granitic rocks (Xiang et al. 2011,
46
47 350 Kirkland et al 2015). The discernible differences in Th/U suggest hotter conditions for the
48
49 351 Permian zircons formed near Berlengas Archipelago than to the south (Fig. 5), which can
50
51 352 be ascribed, for example, to crystallization in a crustal block with previously emplaced mafic
52
53 353 rocks or in a specially thinned lithosphere. Regardless the actual explanation for the
54
55 354 differences in Th/U ratios, these results, coupled with zircon ages, indicate that major
56
57
58
59
60
61
62
63
64
65

355 basement boundaries were cut by the broadly N-S rift structures that control the western
1 border of the LB (Fig. 7).
2
3
4

5 357

8 358 **Conclusions**

10 359 Detrital zircons contained in sedimentary rocks of the Lusitanian Basin with a western
11 provenance yielded either dominant late Cryogenian to Ediacaran ages (Pan-African and/or
12 Cadomian with peaks at 608-554 Ma) or Carboniferous to Permian ages (Variscan and
13 post-Variscan, with peaks at 315-292 Ma). Differences in age signatures and zircon
14 chemistry (Th/U ratios) indicate significant variability along basin-strike in exhumed
15 basement rocks. A discernible peak at ~264 Ma reveals a middle to late Permian thermal
16 event in restricted areas of West Iberia. Although rare, Middle Triassic zircon grains were
17 identified in different regions of the Lusitanian Basin, suggesting that the Triassic rifting was
18 then affecting wide western areas.
19
20
21
22
23
24
25
26
27
28
29
30

31 368 The detrital-zircon signatures of these west-derived strata do not allow a clear diagnosis
32 about the geotectonic nature of the Lusitanian Basin basement. But suggest that: (1) the
33 basin stands on different terranes of the Iberian Massif in its western edge; (2) the
34 Lusitanian Basin developed after the collapse of the Variscan Orogen in an area
35 characterized by recently emplaced igneous rocks (i.e., during the latest Pennsylvanian-
36 Permian); (3) primary zircon sources were more extensively eroded from the western
37 shoulders of the basin, probably due to a combination of crustal thinning and regional
38 eastward basement tilt.
39
40
41
42
43
44
45
46
47
48
49

50 376

53 377 **Acknowledgments**

54
55
56 378 The research was supported by national funds through FCT - Foundation for Science and
57 Technology, I.P., within the scope of the project UIDB/04292/2020 (MARE). Two
58
59

380 anonymous reviewers are acknowledged for their constructive comments and suggestions
1
2 381 that helped to improve the article.
3

4
5 382 **Conflict of interests:** On behalf of all authors, the corresponding author states that there
6
7 383 is no conflict of interest.
8
9

10 384

11 12 13 385 **References**

14
15
16 386 Almeida N, Egydio Silva M, Fonseca PE, Bezerra MH, Basei M, Chaminé HI, Tassinari C
17 387 (2014) Novos dados geocronológicos do Finisterra. *Comunicações Geológicas*
18 388 101:31-34

19
20
21 389 Alves TM, Gawthorpe RL, Hunt DH, Monteiro JH (2002) Jurassic tectono-sedimentary
22 390 evolution of the Northern Lusitanian Basin (offshore Portugal), *Mar. Pet. Geol.*
23 391 19:727–754

24
25
26 392 Alves TM, Gawthorpe RL, Hunt DW, Monteiro JH (2003a) Post-Jurassic tectono-
27 393 sedimentary evolution of the Northern Lusitanian basin (Western Iberian margin).
28 394 *Basin Res* 15:227–250

29
30
31 395 Alves TM, Manuppella G, Gawthorpe RL, Hunt DW, Monteiro JH (2003b) The depositional
32 396 evolution of diapir- and fault-bounded rift basins: Examples from the Lusitanian
33 397 Basin (Offshore Portugal). *Marine and Petroleum Geology* 19:727–754

34
35
36 398 Alves TM, Moita C, Sandnes F, Cunha T, Monteiro JH, Pinheiro LM (2006) Mesozoic–
37 399 Cenozoic evolution of North Atlantic continental-slope basins: The Peniche basin,
38 400 western Iberian margin. *AAPG Bulletin* 90:31-60

39
40
41 401 Arche A, López-Gómez J (1996) Origin of the Permian-Triassic Iberian Basin, central-
42 402 eastern Spain. *Tectonophysics* 266: 443–464

43
44
45 403 Arche A, López-Gómez J, Marzo M, Vargas H (2004) The siliciclastic Permian-Triassic
46 404 deposits in Central and Northeastern Iberian Peninsula (Iberian, Ebro and Catalan
47 405 Basins): A proposal for correlation. *Geol. Acta* 2: 305–320

48
49
50 406 Arenas R, Fernández RD, Pascual FJR, Martínez SS, Parra LMM, Matas J, ... Garcia-
51 407 Casco A. (2016) The Galicia–Ossa-Morena Zone: proposal for a new zone of the
52 408 Iberian Massif. *Variscan implications. Tectonophysics* 681:135-143
53
54
55
56
57
58
59
60
61
62
63
64
65

- 409 Azerêdo AC (1998). Geometry and facies dynamics of Middle Jurassic carbonate ramp
1 410 sandbodies, West-Central Portugal. In: Wright V.P. and Burchette, T. (Eds.):
2 411 Carbonate Ramps. *Geological Society of London*, Special Publications 149, 281-
3 412 314.
- 4 413 Azerêdo AC, Duarte LV, Henriques MH, Manuppella G (2003) Da dinâmica continental no
5 414 Triásico aos mares do Jurássico Inferior e Médio. *Cadernos de Geologia de*
6 415 *Portugal*, Instituto Geológico e Mineiro
- 7 416 Barata J, Duarte LV, Azerêdo AC (2021) Facies types and depositional cyclicity of a
8 417 Toarcian-Aalenian(?) carbonate-siliciclastic mixed succession (Cabo Carvoeiro
9 418 Formation) in the Lusitanian Basin, Portugal. *Journal of Iberian Geology*.
10 419 <https://doi.org/10.1007/s41513-021-00163-2>
- 11 420 Bernet M, van der Beek P, Pik R, Huyghe P, Mugnier JL, Labrin,E, Szulc A (2006)
12 421 Miocene to recent exhumation of the central Himalaya determined from combined
13 422 detrital zircon fission-track and U/Pb analysis of Siwalik sediments, western Nepal.
14 423 *Basin Research* 18:393-412
- 15 424 Dias G, Leterrier J, Mendes A, Simões PP, Bertrand JM (1998) U-Pb zircon and monazite
16 425 geochronology of post-collisional Hercynian granitoids from the Central Iberian
17 426 Zone (northern Portugal). *Lithos* 45:349–369
- 18 427 Dickinson W R (1985) Interpreting provenance relations from detrital modes of
19 428 sandstones. In *Provenance of arenites* (pp. 333-361). Springer, Dordrecht
- 20 429 Díez Fernández R, Arenas R (2015) The Late Devonian Variscan suture of the Iberian
21 430 Massif: A correlation of high-pressure belts in NW and SW Iberia. *Tectonophysics*
22 431 654:96-100
- 23 432 Díez Fernández R, Arenas R, Pereira MF, Sánchez-Martínez S, Albert R, Parra LMM, ...
24 433 Matas J (2016) Tectonic evolution of Variscan Iberia: gondwana–Laurussia
25 434 collision revisited. *Earth-Science Reviews* 162:269-292
- 26 435 Dinis J, Rey J, Cunha PP, Callapez P, Pena dos Reis R (2008) Stratigraphy and allogenic
27 436 controls of the western Portugal Cretaceous: an updated synthesis. *Cretaceous*
28 437 *Research* 29:772-780. doi: 10.1016/j.cretres.2008.05.027
- 29 438 Dinis PA, Dinis J, Tassinari C, Carter A., Callapez P, Morais M (2016) Detrital zircon
30 439 geochronology of the Cretaceous succession from the Iberian Atlantic Margin:
31 440 palaeogeographic implications. *International Journal of Earth Sciences* 105:727-
32 441 745

- 442 Dinis PA., Fernandes P, Jorge RC, Rodrigues B, Chew DM, Tassinari CG (2018) The
1 443 transition from Pangea amalgamation to fragmentation: constraints from detrital
2 444 zircon geochronology on West Iberia paleogeography and sediment sources.
3 445 *Sedimentary Geology* 375:172-187
4
5
6
7 446 Dinis P, Anderson T, Machado G, Guimaraes F (2012) Detrital zircon U–Pb ages of a late-
8 447 Variscan Carboniferous succession associated with the Porto–Tomar shear zone
9 448 (West Portugal): Provenance implications. *Sedimentary Geology* 273–274:19–29
10
11
12 449 Duarte LV (1997). Facies analysis and sequential evolution of the Toarcian-Lower
13 450 Aalenian series in the Lusitanian Basin (Portugal). *Comunicações do Instituto*
14 451 *Geológico e Mineiro* 83: 65–94.
15
16
17
18 452 Duarte LV, Silva RL, Félix F, Comas-Rengifo MJ, da Rocha RB, Mattioli E, et al. (2017)
19 453 The Jurassic of the Peniche Peninsula (Portugal): scientific, education and science
20 454 popularization relevance. *Revista de la Sociedad Geológica de España* 30: 55–70.
21
22
23 455 Duarte LV, Silva RL., Mendonça Filho JG, Poças Ribeiro N., Chagas RBA (2012) High-
24 456 resolution stratigraphy, palynofacies and source rock potential of the Água de
25 457 Madeiros Formation (Lower Jurassic), Lusitanian Basin, Portugal. *Journal of*
26 458 *Petroleum Geology* 35, 105-126
27
28
29
30
31 459 Duarte LV, Soares, AF (2002) Litostratigrafia das séries margo-calcárias do Jurássico
32 460 Inferior da Bacia Lusitânica (Portugal). *Comunicações do Instituto Geológico e*
33 461 *Mineiro* 89: 135–154
34
35
36
37 462 Ellwood PM (1987) Sedimentology of the Upper Jurassic Abadia formation and its
38 463 equivalents, Lusitanian Basin, Portugal. PhD Thesis, Open University, Milton
39 464 Keynes, U.K. (unpublished)
40
41
42
43 465 Fernández-Suárez J, Dunning GR, Jenner GA, Gutiérrez-Alonso G (2000) Variscan
44 466 collisional magmatism and deformation in NW Iberia: constraints from U-Pb
45 467 geochronology of granitoids. *Journal of the Geological Society* 157:565–576
46
47
48
49 468 Fonseca P, Munhá J, Pedro J, Rosas F, Moita P, Araújo A, Leal N (1999) Variscan
50 469 ophiolites and high-pressure metamorphism in southern Iberia. *Ophioliti* 24:259–268
51
52
53 470 Freire-de-Andrade C (1937) Os Vales Submarinos Portugueses e o Diastrofismo das
54 471 Berlengas e da Estremadura. *Memórias dos Serviços Geológicos de Portugal* 5:1-
55 472 35
56
57
58
59
60
61
62
63
64
65

- 473 Gardien V, Paquette JL (2004) Ion microprobe and ID-TIMS U–Pb dating on zircon grains
1 474 from leg 173 amphibolites: evidence for Permian magmatism on the West Iberian
2 margin. *Terra Nova* 16:226–231
3 475
4
- 5 476 Garzanti E (2016) From static to dynamic provenance analysis—Sedimentary petrology
6 uUJ-Graded. *Sedimentary Geology* 336:3-13
7 477
8
- 9 478 Gehrels G (2014) Detrital zircon U-Pb geochronology applied to tectonics. *Annual Review*
10 of Earth and Planetary Sciences 42:127-149
11 479
12
- 13 480 Granado C, Muñoz- Martín A, Olaiz AJ, Fernández O, Druet M (2021) 3D crustal- scale
14 structure of the West Iberia margin: a novel approach to integrated structural
15 481 characterization of passive margins. *Marine Geophysical Research* 42:10
16 482
17 483 <https://doi.org/10.1007/s11001-021-09432-2>
18
19
- 20 484 Griffin WL, Powell WJ, Pearson NJ, O'Reilly SY (2008) GLITTER: data reduction software
21 for laser ablation ICP-MS. In Sylvester P (eds) *Laser Ablation–ICP–MS in the*
22 485 *Earth Sciences*. Mineralogical Association of Canada Short Course Series 40, pp
23 486 204–207
24
25 487
- 26 488 Guéry F, Montenat C, Vachard D (1986) Evolution tectono-sédimentaire du bassin
27 portugais au Mésozoïque suivant la transversale de Peniche (Estremadure).
28 489 *Bulletin des centres de recherches exploration-Production Elf-Aquitaine* 10:83-94
29
30 490
31
- 32 491 Gutiérrez-Alonso G, Fernández-Suárez J., Jeffries TE, Johnston ST, Pastor-Galán D,
33 Murphy JB, Franco MP, Gonzalo JC (2011) Diachronous post-orogenic
34 492 magmatism within a developing orocline in Iberia, European Variscides. *Tectonics*
35 493 30, TC5008. <https://doi.org/10.1029/2010TC002845>
36
37 494
38
- 39 495 Gutiérrez-Alonso G, Fernández-Suárez J, Weil AB (2004) Orocline triggered lithospheric
40 delamination. *Geological Society America Special Papers* 383:121–130
41 496
42
- 43 497 Hawkesworth C, Cawood P, Dhuime B (2013) Continental growth and the crustal record:
44 Tectonophysics 609:651–660, [j.tecto.2021.228863](https://doi.org/10.1016/j.tecto.2021.228863)
45 498
46
- 47 499 Hildenbrand A, Marques FO, Quidelleur X, Noronha F (2021) Exhumation history of the
48 Variscan orogen in western Iberia as inferred from new KAr and 40Ar/39Ar data on
49 500 granites from Portugal. *Tectonophysics*, 228863.
50 501
51
- 52 502 Hill G (1989) Distal alluvial fan sediments from the Upper Jurassic of Portugal: controls on
53 503 their cyclicity and channel formation. *J Geol Soc London* 146:539–555.
54
55
56
57
58
59
60
61
62
63
64
65

- 504 Hutter AD, Beranek LP (2020) Provenance of Upper Jurassic to Lower Cretaceous synrift
1 strata in the Terra Nova oil field, Jeanne d'Arc basin, offshore Newfoundland: A
2
3 506 new detrital zircon U-Pb-Hf reference frame for the Atlantic Canadian margin.
4
5 507 AAPG Bulletin, 104:2325-2349
6
- 7 508 Jesus A, Munhá J, Mateus A, Tassinari C, Nutman A (2007) The Beja layered gabbroic
8
9 509 sequence (Ossa–Morena Zone, Southern Portugal): geochronology and
10
11 510 geodynamic implications. *Geodinamica Acta* 20:139–157
12
- 13 511 Julivert M, Fontboté JM, Ribeiro A, Conde LEN (1974) Mapa Tectónico de la Península
14
15 512 Ibérica y Baleares, Escala 1:1000.000. Memória Explicativa. Instituto Geologico y
16
17 513 Minero de España, Madrid.
18
- 19 514 Kirkland CL, Smithies RH, Taylor RJM, Evans N, McDonald B (2015) Zircon Th/U ratios in
20
21 515 magmatic environs. *Lithos* 212:397-414
22
- 23 516 Kullberg, J. C., & Rocha, R. B. (2014). O Jurássico Superior da Bacia Lusitaniana:
24
25 517 importância da ligação entre litostratigrafia, cronostratigrafia e cartografia. I-O final
26
27 518 do 2º episódio de rifting. *Comunicações Geológicas*, 101(Especial I), 459-462.
28
- 29 519 Kullberg JC, Rocha RB, Soares AF, Rey J, Terrinha P, Azerêdo AC, Callapez P, Duarte
30
31 520 LV, Kullberg MC, Martins L, Miranda JR, Alves C, Mata J, Madeira J, Mateus O,
32
33 521 Moreira M. (2013). A Bacia Lusitaniana: Estratigrafia, Paleogeografia e Tectónica.
34
35 522 In R. Dias, A. Araujo, P. Terrinha, & J.C. Kullberg (Eds.), *Geologia de Portugal no*
36
37 523 *contexto da Ibéria. Vol. II - Geologia Meso-cenozóica de Portugal* (pp. 195–347).
38
39 524 Livr. Escolar Editora
40
- 41 525 Leinfelder RR, Wilson RCL (1998) Third-order sequences in an Upper Jurassic rift-related
42
43 526 second-order sequence, central Lusitanian basin, Portugal. In: Graciansky PC,
44
45 527 Hardenbol J, Jacquin T, Vail PR (eds) *Mesozoic and cenozoic sequence*
46
47 528 *stratigraphy of European basins*, SEPM Spec Pub 60:507–525
48
- 49 529 Linnemann U, Pereira MF, Jeffries T, Drost K, Gerdes A (2008) Cadomian Orogeny and
50
51 530 the opening of the Rheic Ocean: the diachrony of geotectonic processes
52
53 531 constrained by LA-ICP-MS U–Pb zircon dating (Ossa-Morena and Saxo-
54
55 532 Thuringian Zones, Iberian and Bohemian Massifs). *Tectonophysics* 461:21–43
56
- 57 533 López-Gómez, J, Martín-González F, Heredia N, De la Horra R, Barrenechea JF,
58
59 534 Cadenas P, Juncal M, Díez JB, Borrueal-Abadia V, Pedreira D, García-Sansegundo
60
61 535 J, Farias P, Galé C, Lago M, Ubide T, Fernández-Viejo G, Gand G (2019) New
62
63 536 lithostratigraphy for the Cantabrian Mountains: A common tectonostratigraphic
64
65

- 537 evolution for the onset of the Alpine cycle in the W Pyrenean realm, N Spain. *Earth*
1 538 *Sciences Review* 188:249–271
2
3
4 539 López-Gómez J, De la Horra R, Barrenechea JF, Borrueal-Abadía V, Martín-Chivelet J,
5 540 Juncal M, Martín-González F, Heredia F, Diez JB, Buatois LA (2021) Early
6 541 Permian during the Variscan Orogen Collapse in the equatorial realm: insights
7 542 from the Cantabrian Mountains (N Iberia) into climatic and environmental changes.
8 543 *International Journal of Earth Sciences*. doi.org/10.1007/s00531-021-02020-0
9
10
11
12 544 Lowe DG, Sylvester PJ, Enachescu ME (2011) Provenance and paleodrainage patterns of
13 545 Upper Jurassic and Lower Cretaceous synrift sandstones in the Flemish Pass
14 546 Basin, offshore Newfoundland, east coast of Canada. *AAPG Bulletin* 95:1295–
15 547 1320
16
17
18
19
20 548 MacLean NJ, Barr SM, White CE, Ketchum JW (2003) New U-Pb (zircon) age and
21 549 geochemistry of the Wedgeport Pluton, Meguma terrane, Nova Scotia. *Atlantic*
22 550 *Geology* 39:239–253
23
24
25
26 551 Malusà MG., Garzanti E (2019) The sedimentology of detrital thermochronology.
27 552 In *Fission-Track Thermochronology and its Application to Geology*, pp. 123-143..
28 553 Springer, Cham.
29
30
31 554 Marques B, Oloriz F, Caetano PS, Rocha RB, Kullberg JC (1992) Upper Jurassic of the
32 555 Alcobaça Region. *Stratigraphic Contributions. Comunicações dos Serviços*
33 556 *Geológicos de Portugal* 78:63-69
34
35
36
37 557 Marques FO, Mateus A, Tassinari C (2002) The Late-Variscan fault network in central–
38 558 northern Portugal (NW Iberia): a re-evaluation. *Tectonophysics* 359:255-270
39
40
41 559 Merino-Tomé O, Bahamonde JR, Colmenero JR, Heredia N, Villa E, Farias P (2009)
42 560 Emplacement of the Cuera and Picos de Europa imbricate system at the core of
43 561 the Ibero-Armorican arc (Cantabrian Zone, N Spain): new precisions concerning
44 562 the timing of arc closure. *Geological Society of America Bulletin* 121:729–751
45
46
47
48
49 563 Moecher DP, Samson SD (2006) Differential zircon fertility of source terranes and natural
50 564 bias in the detrital zircon record: Implications for sedimentary provenance analysis.
51 565 *Earth and Planetary Science Letters* 247:252-266
52
53
54
55 566 Moreira N, Romão J, Dias R, Ribeiro A., Pedro J (2019) The Finisterra-Léon-Mid German
56 567 Crystalline Rise Domain; Proposal of a New Terrane in the Variscan Chain. In *The*
57 568 *Geology of Iberia: A Geodynamic Approach* (pp. 207-228). Springer, Cham.

- 569 Murphy JB, Nance RD (1991) Supercontinent model for the constraining character of Late
1 570 Proterozoic orogenic belts. *Geology* 19:469–472
2
3
4 571 Nance RD, Murphy JB (1994) Contrasting basement isotopic signatures and the
5 572 palinspatic restoration of peripheral orogens: example from the Neoproterozoic
6 573 Avalonian–Cadomian belt. *Geology* 22:617–620
7
8
9 574 Oliveira JT, Pereira E, Ramalho M, Antunes MT, Monteiro JH (1992) Carta geológica de
10 575 Portugal à escala 1/500000, 5a edição (coords.). Serviços Geológicos de Portugal,
11 576 Lisboa
12
13
14
15 577 Orejana D, Villaseca C, Billstrom K, Paterson BA (2008) Petrogenesis of Permian alkaline
16 578 lamprophyres and diabases from the Spanish Central System and their
17 579 geodynamic context within western Europe. *Contrib Miner Petrol* 156:457–500
18
19
20
21 580 Palain C (1976) Une série détritique terrigène les “Grès de Silves”: Trias et Lias inférieur
22 581 du Portugal. *Mem. Serv. Geol. Portugal* 25:1–377.
23
24
25 582 Pastor-Galán D, Gutiérrez-Alonso G, Murphy JB, Fernández-Suárez J, Hofmann M,
26 583 Linnemann U (2013) Provenance analysis of the Paleozoic sequences of the
27 584 northern Gondwana margin in NW Iberia: passive margin to Variscan collision and
28 585 orocline development. *Gondwana Research* 23:1089–1103
29
30
31
32 586 Pe-Piper G, Kamo SL, McCall C (2010) The German Bank pluton, offshore SW Nova
33 587 Scotia: Age, petrology, and regional significance for Alleghanian plutonism.
34 588 *Geological Society of America Bulletin* 122:690–700
35
36
37
38 589 Pena dos Reis R, Cunha PP, Dinis JL, Trincão PR (2000) Geologic evolution of the
39 590 Lusitanian Basin (Portugal) during the Late Jurassic. *GeoResearch Forum*,
40 591 *Transtec Publications, Zurich*, vol. 6; 345-356
41
42
43
44 592 Pena dos Reis R, Dinis J, Cunha PP, Trincão P (1996) Upper Jurassic sedimentary infill
45 593 and tectonics of the Lusitanian Basin (Western Portugal). In *Jurassic Research*,
46 594 Editor: A.C. Riccardi. *GeoResearch Forum, Transtec Publications, Zurich*, vols. 1-
47 595 2:377-386
48
49
50
51 596 Pereira MF, Chichorro M, Johnston ST, Gutiérrez-Alonso G, Silva JB, Linnemann U,
52 597 Hofmann M, Drost K (2012b) The missing Rheic Ocean magmatic arcs:
53 598 provenance analysis of Late Paleozoic sedimentary clastic rocks of SW Iberia.
54 599 *Gondwana Res* 3–4:882–891
55
56
57
58
59 600 Pereira MF, Linnemann U, Hofmann M, Chichorro M, Solá AR, Medina J, Silva JB (2012a)
60 601 The provenance of Late Ediacaran and Early Ordovician siliciclastic rocks in the
61
62
63
64
65

- 602 Southwest Central Iberian Zone: constraints from detrital zircon data on northern
1 603 Gondwana margin evolution during the late Neoproterozoic. *Precambr Res* 192–
2 604 195:166–189
3
4
5 605 Pereira MF, Gama C, Silva JB, da Silva ÍD (2020) Age of the basement beneath the
6
7 606 Mesozoic Lusitanian Basin revealed by granitic xenoliths from the Papôa volcanic
8
9 607 breccia (West Iberia). *Geologica Acta* 18:1-14
10
11 608 Pereira MF, Ribeiro C, Vilallonga F, Chichorro M, Drost K, Silva JB, Albardeiro L, Hofman
12
13 609 M, Linnemann U (2014) Variability over time in the sources of South Portuguese
14
15 610 Zone turbidites: evidence of denudation of different crustal blocks during the
16
17 611 assembly of Pangaea. *International Journal of Earth Sciences* 103:1453-1470
18
19 612 Pereira MF, Gama C, Chichorro M, Silva JB, Gutiérrez-Alonso G, Hofmann M, Linnemann
20
21 613 U, Gartner A (2016) Evidence for multi-cycle sedimentation and provenance
22
23 614 constraints from detrital zircon U–Pb ages: Triassic strata of the Lusitanian basin
24
25 615 (western Iberia). *Tectonophysics* 681:318–331
26
27 616 Pereira MF, Ribeiro C, Gama C, Drost K, Chichorro M, Vilallonga F, Hofmann M,
28
29 617 Linnemann U (2017) Provenance of upper Triassic sandstone, southwest Iberia
30
31 618 (Alentejo and Algarve basins): tracing variability in the sources. *International*
32
33 619 *Journal of Earth Sciences* 106:43–57
34
35 620 Pereira R, Alves TM, Mata J (2017) Alternating crustal architecture in West Iberia: a
36
37 621 review of its significance in the context of NE Atlantic rifting. *J Geol Soc Lond Spec*
38
39 622 *Publ* 174:522–540
40
41 623 Pinheiro L, Wilson R, Reis RP, Whitmarsh R, Ribeiro A (1996) The western Iberia margin:
42
43 624 a geophysical and geological overview. *Proc Ocean Drill Program Sci Res* 149:3–
44
45 625 23
46
47 626 Priem HNA, Boelrijk NAIM, Verschure RH, Hebeda EH (1965) Isotopic ages of two
48
49 627 granites on the Iberian continental margin: The Traba Granite (Spain) and the
50
51 628 Berlenga Granite (Portugal). *Geologie en Mijnbouw* 10:353–354
52
53 629 Quesada C (1991) Geological constraints on the Paleozoic tectonic evolution of
54
55 630 tectonostratigraphic terranes in the Iberian Massif, *Tectonophysics* 185, 225–245.
56
57 631 Rasmussen ES, Lomholt S, Andersen C, Vejbæk OV (1998) Aspects of the structural
58
59 632 evolution of the Lusitanian Basin in Portugal and the shelf and slope area offshore
60
61 633 Portugal. *Tectonophysics* 300: 199-225.
62
63
64
65

- 634 Ravnås R, Windelstad J, Mellere D, Nøttvedt A., Sjøblom TS, Steel RJ, Wilson RCL
1 635 (1997) A marine Late Jurassic syn-rift succession in the Lusitanian Basin, western
2 636 Portugal—tectonic significance of stratigraphic signature. *Sedimentary Geology*
3 637 114:237-266
4
5
6
7 638 Ribeiro A, Munhá J, Dias R, Mateus A, Pereira E, Ribeiro L, Fonseca PE, Araújo A,
8 639 Oliveira JT, Romão J, Chaminé HI, Coke C, Pedro JC (2007) Geodynamic
9 640 evolution of the SW Europe Variscides. *Tectonics* 26 (6):TC6009
10 641 <https://doi.org/10.1029/2006tc002058>.
11
12
13
14 642 Ribeiro A, Quesada C, Dallmeyer RD (1990) Geodynamic evolution of the Iberian Massif.
15 643 In: Dallmeyer, R.D., Martínez-García, E. (Eds.), *Pre-Mesozoic Geology of Iberia*.
16 644 Springer Verlag, Berlin, Heidelberg, pp. 397–410
17
18
19
20 645 Rino S, Komiya T, Windley BF, Katayama I, Motoki A, Hirata T (2004) Major episodic
21 646 increases of continental crustal growth determined from zircon ages of river sands
22 647 implications for mantle overturns in the Early Precambrian: *Physics of the Earth*
23 648 and Planetary Interiors, v. 146, p. 369–394, doi:10.1016/j.pepi.2003.09.024
24
25
26
27 649 Rodrigues B, Chew DM, Jorge RCGS, Fernandes P, Veiga-Pires C, Oliveira JT (2015)
28 650 Detrital zircon geochronology of the Carboniferous Baixo Alentejo Flysch Group
29 651 (South Portugal); constraints on the provenance and geodynamic evolution of the
30 652 South Portuguese Zone. *Journal of the Geological Society* 172(3):294-308
31
32
33
34
35 653 Schneider S, Fürsich FT, Werner W (2009). Sr-isotope stratigraphy of the Upper Jurassic
36 654 of central Portugal (Lusitanian Basin) based on oyster shells. *International Journal*
37 655 *of Earth Sciences* 98:1949-1970
38
39
40
41 656 Shaw J, Gutiérrez-Alonso G, Johnston ST, Galán DP (2014). Provenance variability along
42 657 the Early Ordovician north Gondwana margin: Paleogeographic and tectonic
43 658 implications of U-Pb detrital zircon ages from the Armorican Quartzite of the
44 659 Iberian Variscan belt. *GSA Bulletin* 126:702-719
45
46
47
48 660 Simancas JF (2019) Variscan Cycle. In: Quesada C., Oliveira J. (eds) *The Geology of*
49 661 *Iberia: A Geodynamic Approach*. Regional Geology Reviews. Springer, Cham.
50 662 https://doi.org/10.1007/978-3-030-10519-8_1
51
52
53
54 663 Simancas JF, Tahiri A, Azor A, Lodeiro FG, Martínez Poyatos DJ, El Hadi H (2005) The
55 664 tectonic frame of the Variscan-Alleghanian orogen in southern Europe and
56 665 northern Africa. *Tectonophysics* 398:181–198
57
58
59
60
61
62
63
64
65

- 666 Soares AF, Kullberg JC, Marques JF, Rocha RB, Callapez P (2012) Tectono-sedimentary
1 667 model for the evolution of the Silves Group (Triassic, Lusitanian basin, Portugal).
2
3 668 Bull Soc Géol France 183 (3):203–216
4
- 5 669 Sousa M, Sant’Ovaia H, Tassinari C, Noronha F. (2014) Geocronologia U-Pb (SHRIMP) e
6
7 670 Sm-Nd do ortognaisse biotítico do Complexo Metamórfico da Foz do Douro (NW
8
9 671 de Portugal). Comunicações Geológicas 101:225-228
10
- 11 672 Stanton N, Manatschal G, Autin J, Sauter D, Maia M, Viana A (2016) Geophysica
12
13 673 Ifingerprints of hyper-extended, exhumed and embryonic oceanic domains:
14
15 674 theexample for the Iberia-Newfoundland rifted margins. Mar Geophys Res.
16
17 675 37:185–205
18
- 19 676 Stapel G, Cloetingh S, Pronk B (1996) Quantitative subsidence analysis of the Mesozoic
20
21 677 evolution of the Lusitanian basin (western Iberian margin). Tectonophysics
22
23 678 266:493-507.
24
- 25 679 Talavera C, Montero P, Martínez Poyatos D, Williams H (2012) Ediacaran to Lower
26
27 680 Ordovician age for rocks ascribed to the Schist Graywacke Complex (Iberian
28
29 681 Massif, Spain): evidence from detrital zircon SHRIMP U–Pb geochronology.
30
31 682 Gondwana Res 22:928–942
32
- 33 683 Taylor AM, Gowland S, Leary S, Keogh KJ, Martinius AW (2014). Stratigraphical
34
35 684 correlation of the Late Jurassic Lourinhã Formation in the Consolação Sub-basin
36
37 685 (Lusitanian Basin), Portugal. Geological Journal 49:143-162
38
- 39 686 Terrinha P. et al. (2019) Rifting of the Southwest and West Iberia Continental Margins. In:
40
41 687 Quesada C., Oliveira J. (eds) The Geology of Iberia: A Geodynamic Approach.
42
43 688 Regional Geology Reviews. Springer, Cham. https://doi.org/10.1007/978-3-030-11295-0_6
44
- 45 690 Valverde-Vaquero P, Bento-dos-Santos T, González-Clavijo E, Díez-Montes A, Ribeiro
46
47 691 ML, Solá AR, Dias-da-Silva Í (2011) The Berlengas Archipelago granitoids within
48
49 692 the frame of the Variscan Orogeny, W Portugal: new data and insights. 7th Hutton
50
51 693 Symposium on Granites and Related Rocks, Ávila, 153
52
- 53 694 Vanney J-R, Mougnot D. (1981) La plate-forme continentale du Portugal et les provinces
54
55 695 adjacentes: analyse geomorphologique. Mem. Serv. Geol. Portugal, 28.
56
- 57 696 Vermeesch P (2012) On the visualisation of detrital age distributions. Chem Geol 312–
58
59 697 313:190–194
60
61
62
63
64
65

- 698 Vermeesch P (2013) Multi-sample comparison of detrital age distributions. *Chem Geol*
699 341:140–146
- 700 Wang W, Zhang P, Yu J, Wang Y, Zheng D, Zheng W., ... Pang J. (2016) Constraints on
701 mountain building in the northeastern Tibet: Detrital zircon records from
702 synorogenic deposits in the Yumen Basin. *Scientific reports* 6(1):1-8
- 703 Wilson RCL (1979) A reconnaissance study of Upper Jurassic sediments of the Lusitanian
704 Basin. *Ciências da Terra* 5:53–84
- 705 Wilson RCL (1989) Mesozoic development of the Lusitanian Basin, Portugal. *Rev. Soc.*
706 *Geol. Esp.* 1:393-407
- 707 Wilson RCL, Hiscott R, Willis M, Gradstein F (1989) The Lusitanian Basin of west central
708 Portugal; Mesozoic and Tertiary tectonic, stratigraphic and subsidence history. In:
709 Tankard, A. & Balkwill, H., *Extensional tectonics and stratigraphy of the North*
710 *Atlantic margins*. AAPG Memoir 46:341–361
- 711 Wright VP, Wilson RCL (1984) A carbonate submarine-fan sequence from the Jurassic of
712 Portugal. *Journal of Sedimentary Research* 54(2):394-412
- 713 Xiang W, Griffin WL, Jie C., Pinyun H, Xiang LI (2011) U and Th contents and Th/U ratios
714 of zircon in felsic and mafic magmatic rocks: Improved zircon-melt distribution
715 coefficients. *Acta Geologica Sinica-English Edition* 85(1):164-174

716 **FIGURES CAPTIONS**

717

718 Fig. 1: Geological framework of the studied deposits. (A) Major tectono-stratigraphic units of the
719 Iberia Massif. CZ: Cantabrian Zone; WALZ: West Asturian-Leonese Zone; GTMZ: Galicia - Trás-
720 os-Montes Zone; CIZ: Central Iberian Zone; OMZ: Ossa Morena Zone; SPZ: South Portuguese
721 Zone. (B) The Lusitanian Basin covering different tectono-stratigraphic units and bounded to the
722 west by the Berlingas Block (BB). (C) Jurassic and basement outliers in central west Iberian
723 margin and location of the sampled sections (black diamonds). PTFZ: Porto-Tomar Fault Zone.
724 Key sites for the Jurassic stratigraphy in the Lusitanian Basin are also indicated. Small grey
725 diamonds indicate the location of other published detrital zircon data for basement (A and B) and
726 Mesozoic (C) units used in this investigation.

727

728 Fig. 2: Stratigraphic framework for the beds sampled in the Lusitania Basin. Based on Rasmussen
729 et al (1998), Pena dos Reis et al. (2000), Duarte and Soares (2002), Azerêdo et al. (2003),
730 Schneider et al. (2009), Kullberg and Rocha (2014).

731

732 Fig. 3: Stratigraphic sections sampled for U-Pb zircon geochronology. Geographic location in Fig. 1
733 and stratigraphic setting in Fig. 2.

734

735 Fig. 4: Pie diagrams and Kernel density plots of detrital zircon ages for Lower and Upper Jurassic
736 units sourced by the Berlingas Block. Shadow areas in the insets for 750-200 Ma represent
737 characteristic zircon forming events already recognized for Cretaceous deposits from the Iberian
738 Atlantic margin (Dinis et al. 2016).

739

740 Fig. 5: Plot of zircon ages and respective Th/U ratios. Note the different Th/U ratios in younger
741 zircons collected in the Toarcian of Peniche (LJ-Ab) and the Kimmeridgian-Tithonian of Praia da
742 Amoreira (UJ-Am).

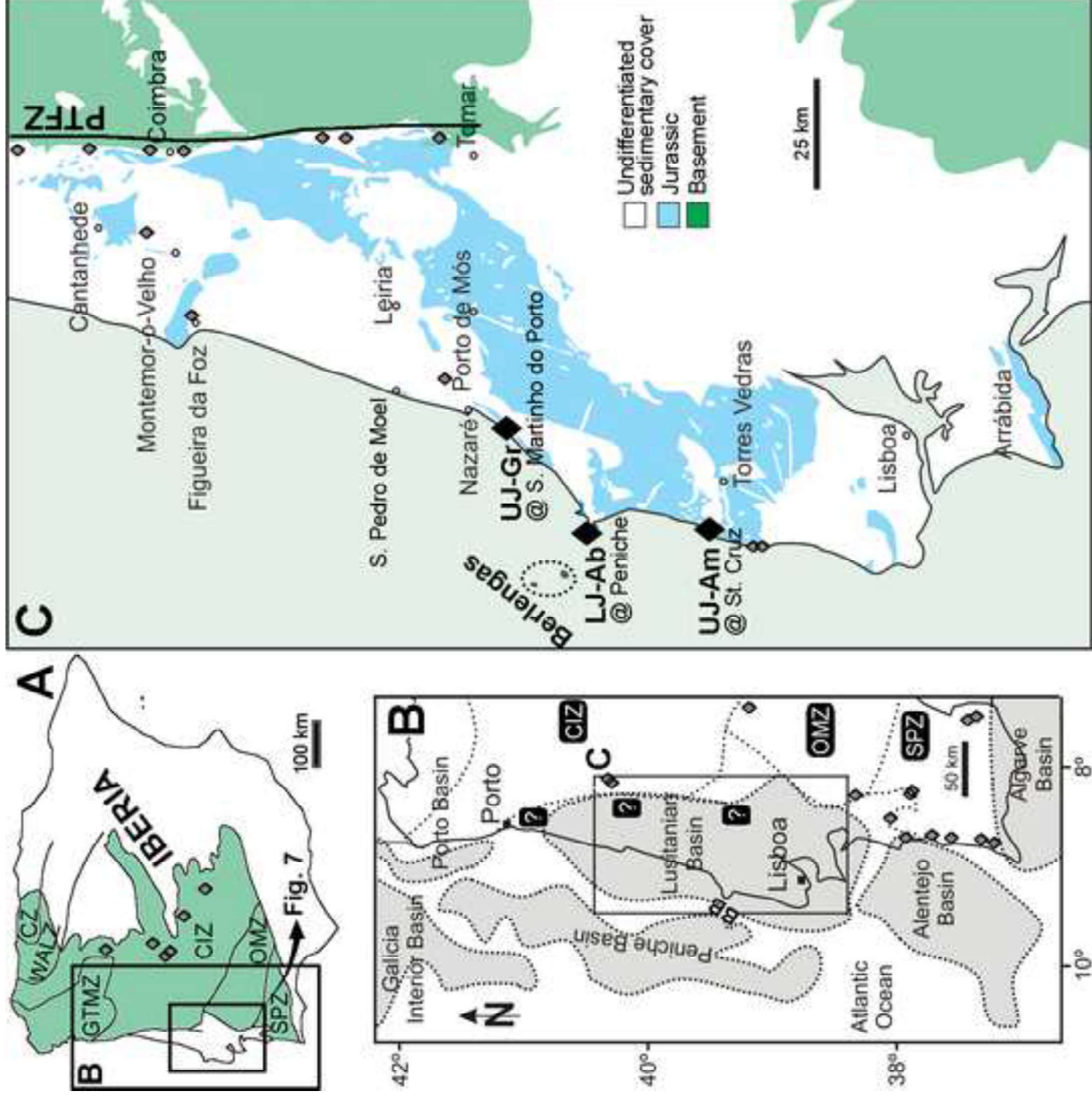
743

744 Fig. 6: MDS map obtained with the detrital zircon age data for the studied deposits and published
745 ages for different terranes that outcrop in West Iberia. The map pulls apart samples with different
746 spectra, using the Kolmogorov Smirnov effect size as a dissimilarity measure (Vermeesch 2013).
747 Basement data for the Central Iberian Zone (CIZ) from Talavera et al. (2012), Pereira et al. (2012a)
748 and Shaw et al (2014); for the Ossa Morena Zone (OMZ) from Linnemann et al. (2008) and Pereira
749 et al. (2012b); for the South Portuguese Zone (SPZ) from Pereira et al. (2012b, 2014) and
750 Rodrigues et al. (2015); for sedimentary successions deposited at the contact OMZ-CIZ in

751 association with the Porto-Tomar Fault Zone (PTF-SS) from Dinis et al. (2012, 2018). One sample
1 752 of OMZ is plotted differently from the main cluster for this zone.

3 753

6 754 Fig. 7: Proposed Variscan basement units in the western edge of the Lusitanian Basin based on
7 755 detrital zircon results. Arrows indicate detrital zircon signatures for different stratigraphic intervals;
8
9 756 main frequency peaks in bold and secondary peaks between brackets. Detrital zircon age results
10 757 for Triassic strata from Pereira et al. (2016) and Dinis et al (2018), and for Cretaceous strata from
11 758 Dinis et al (2016). The inset is a schematic profile depicting an overall basement tilt partially
12 759 responsible for the differences in age signatures between east- and west-derived deposits.



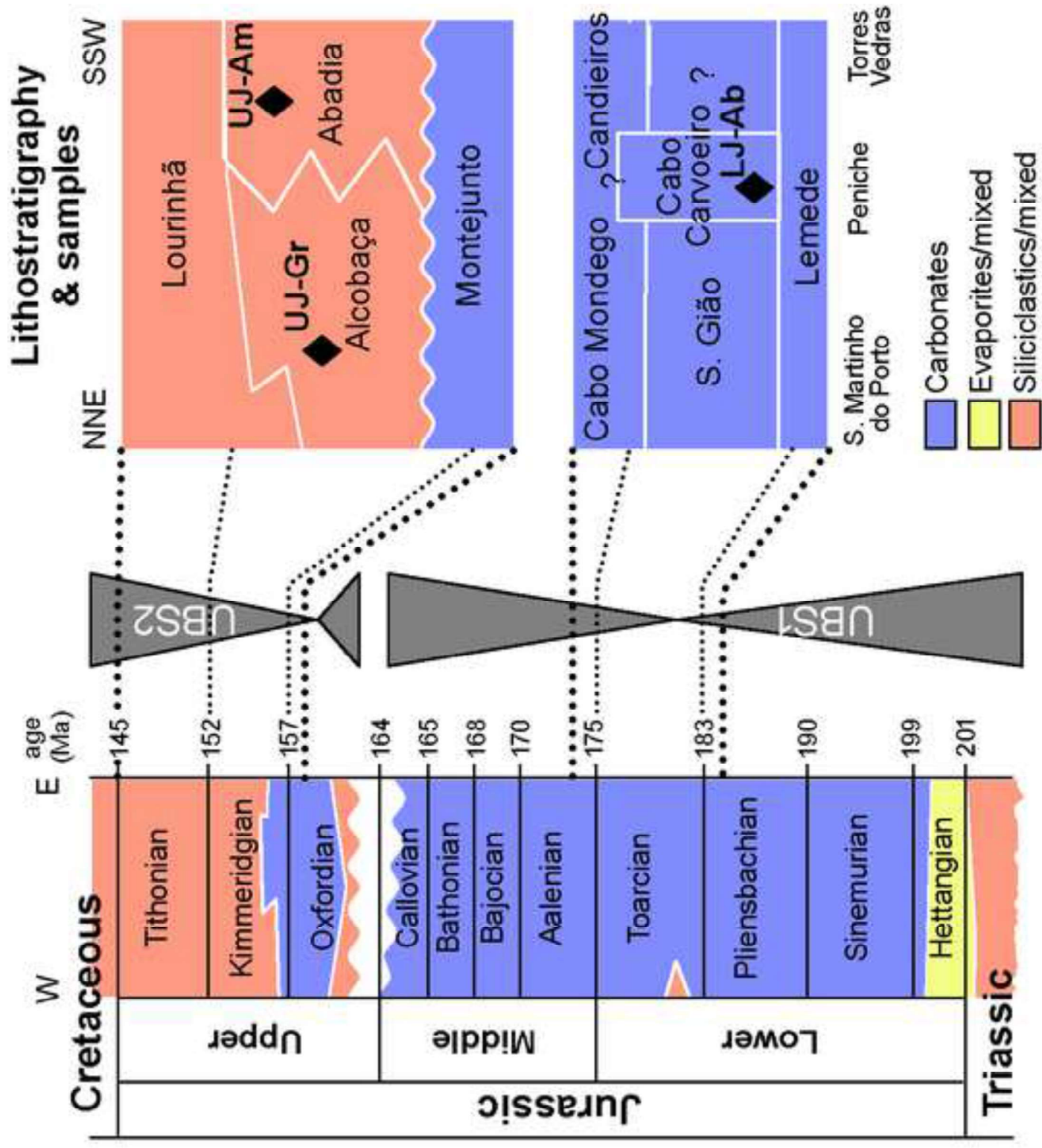


Figure 3

[Click here to access/download;Figure;Fig.3.jpg](#)

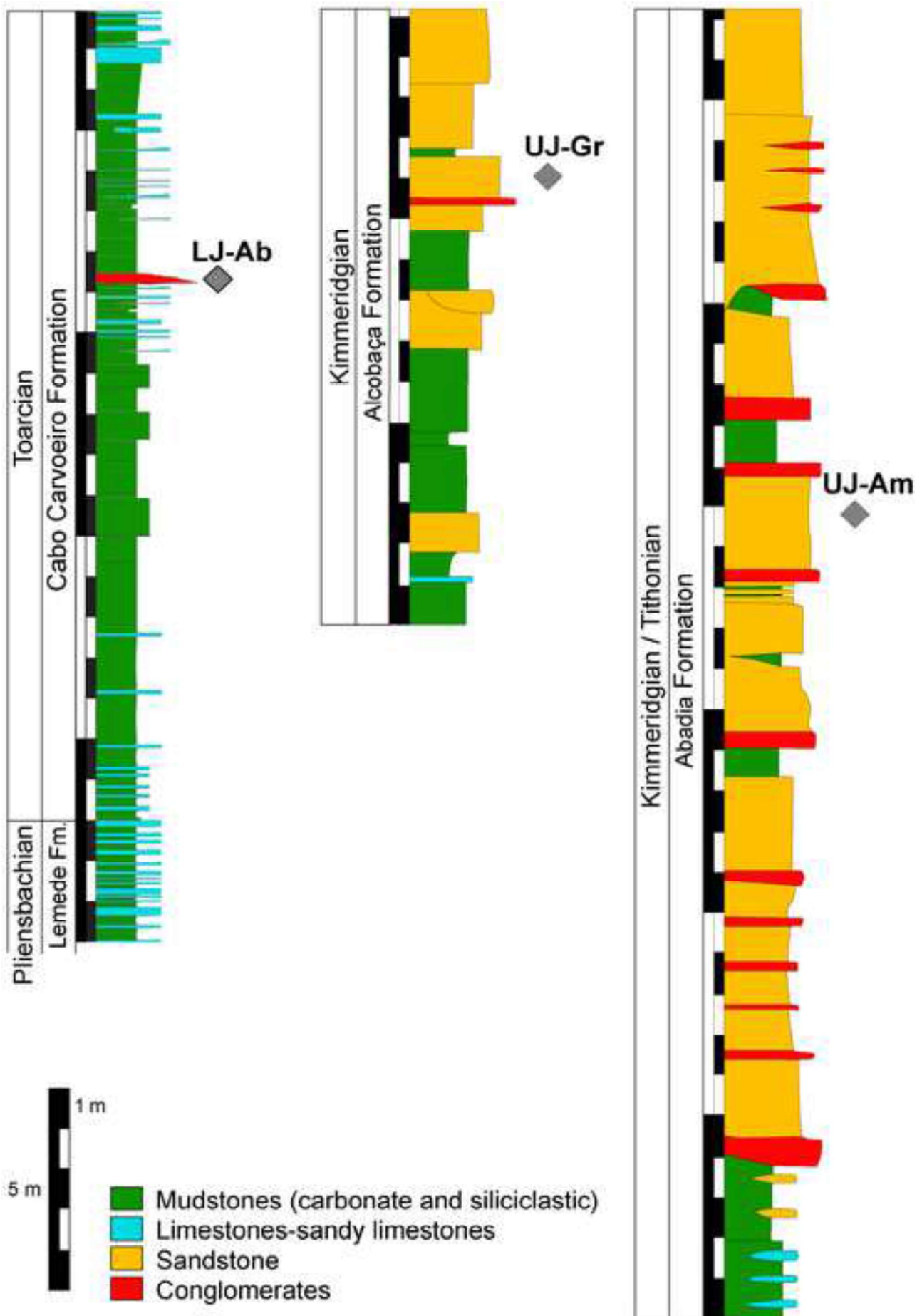


Figure 4

[Click here to access/download;Figure;Fig.4.jpg](#)

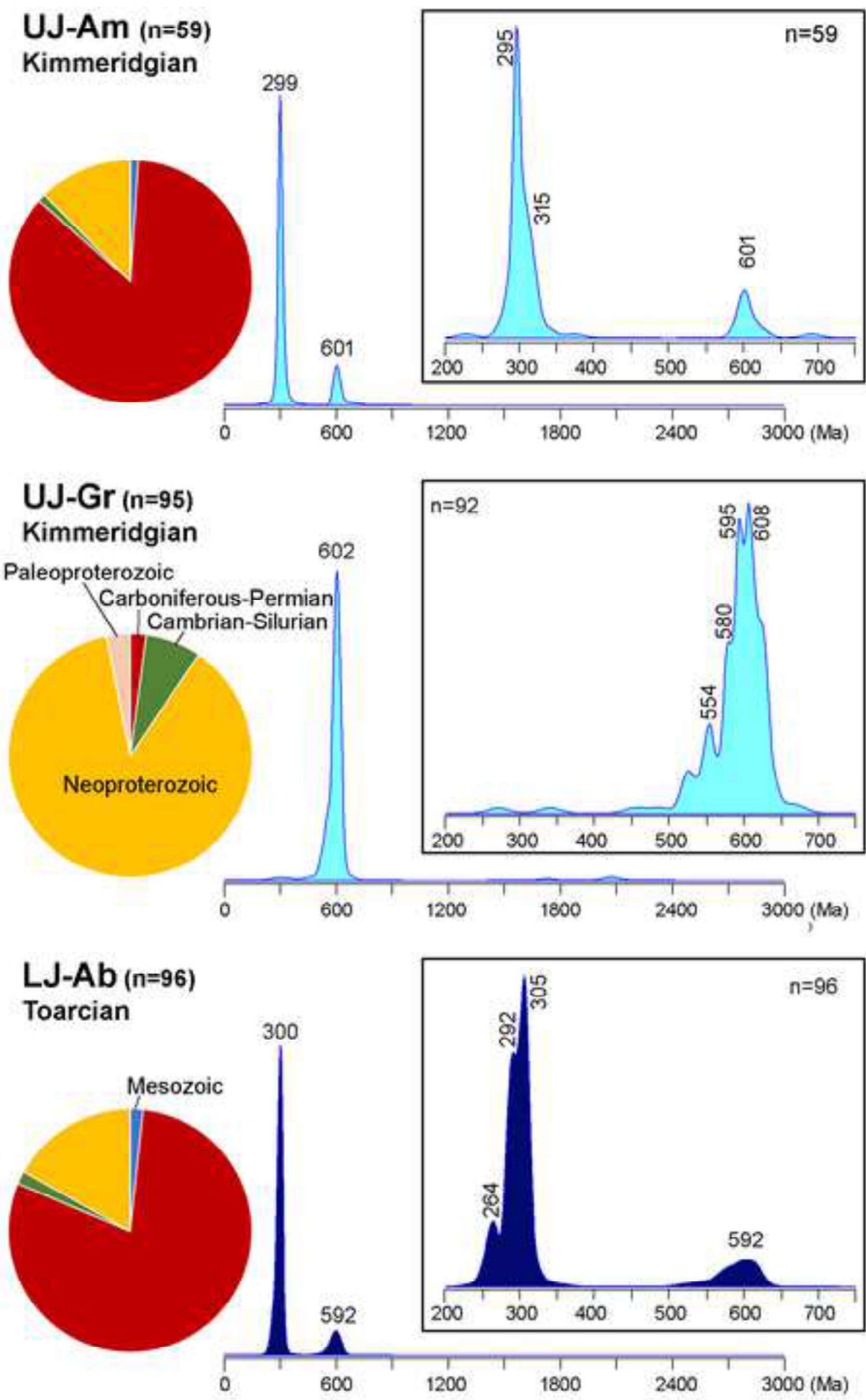
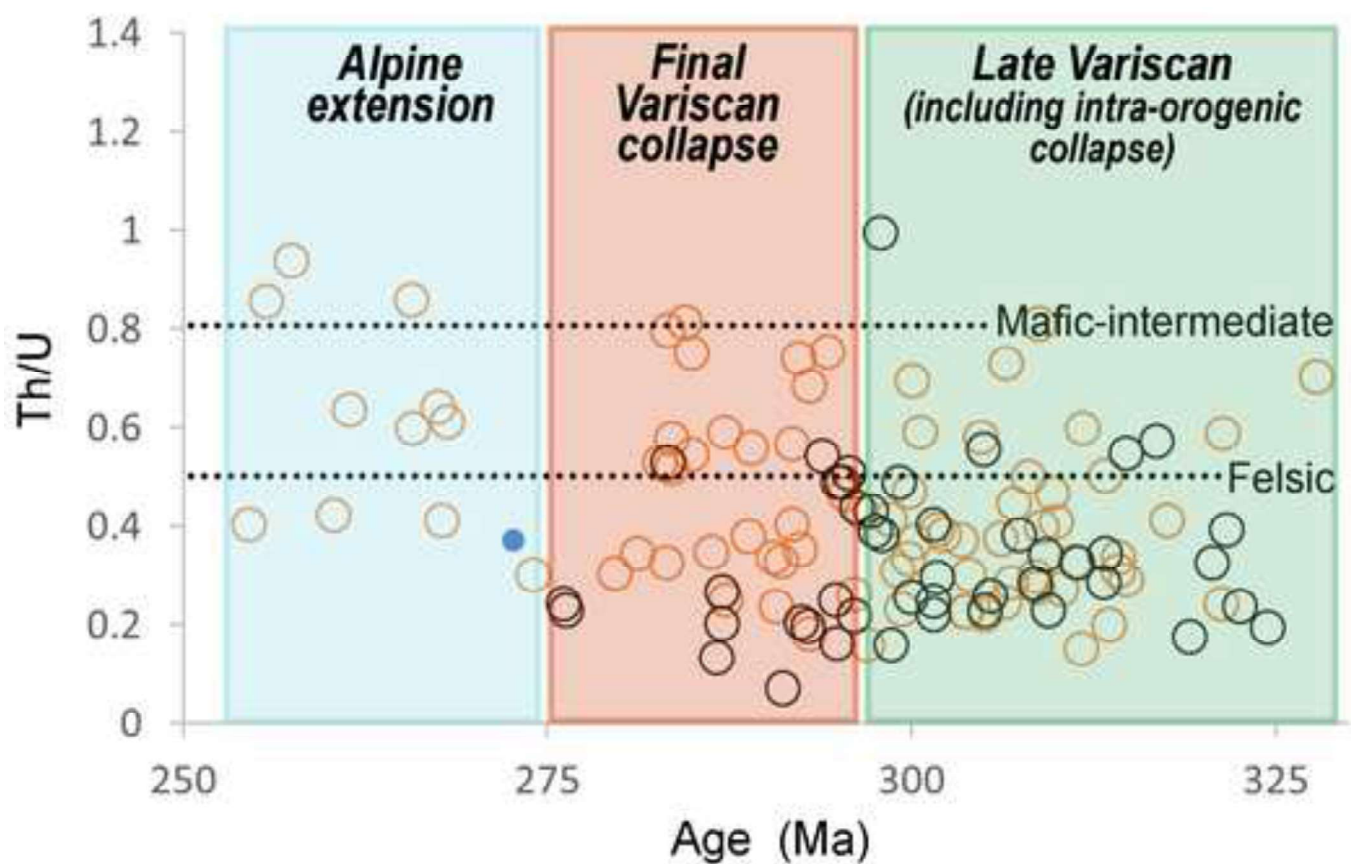
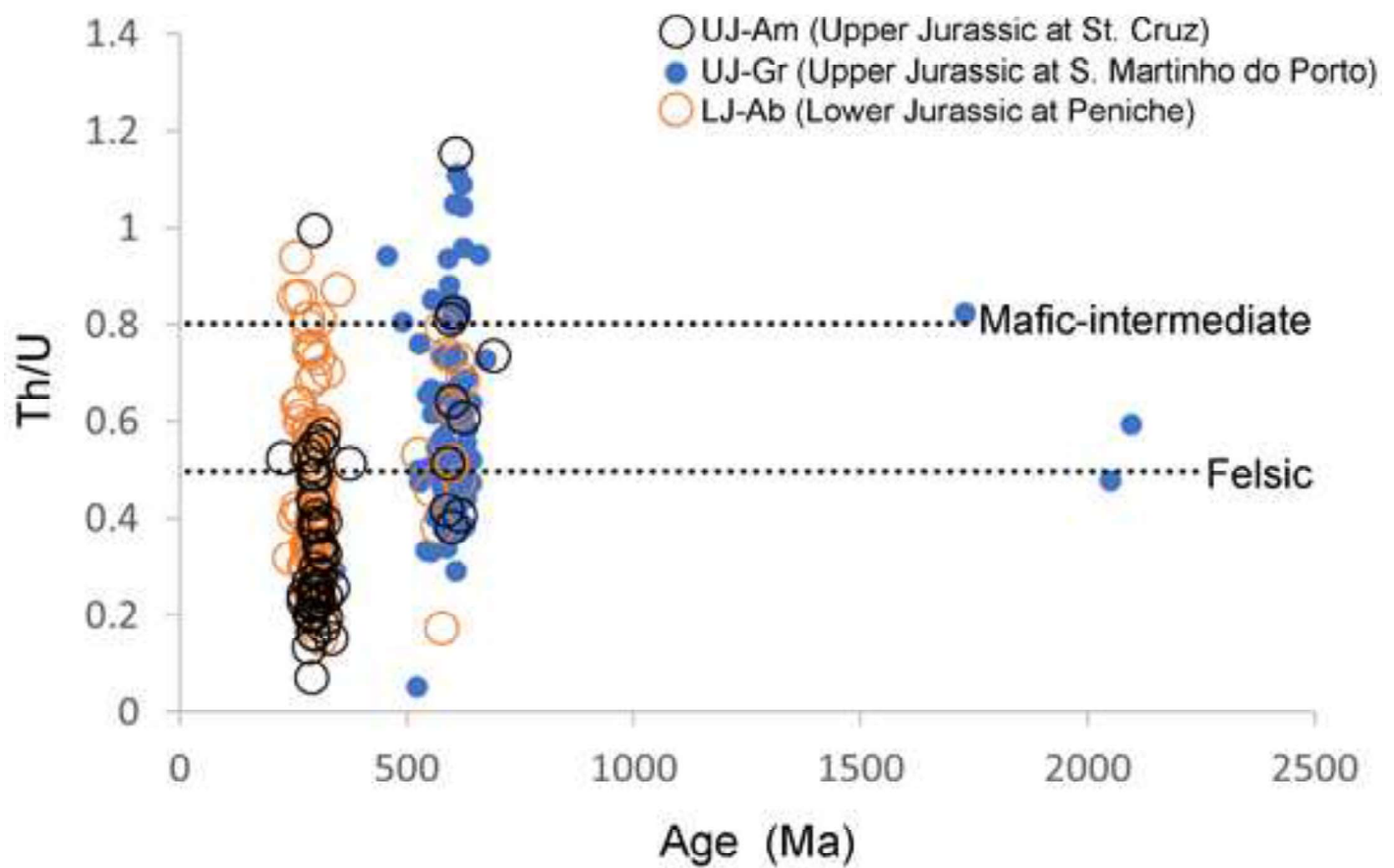


Figure 5

[Click here to access/download;Figure;Fig.5.jpg](#)



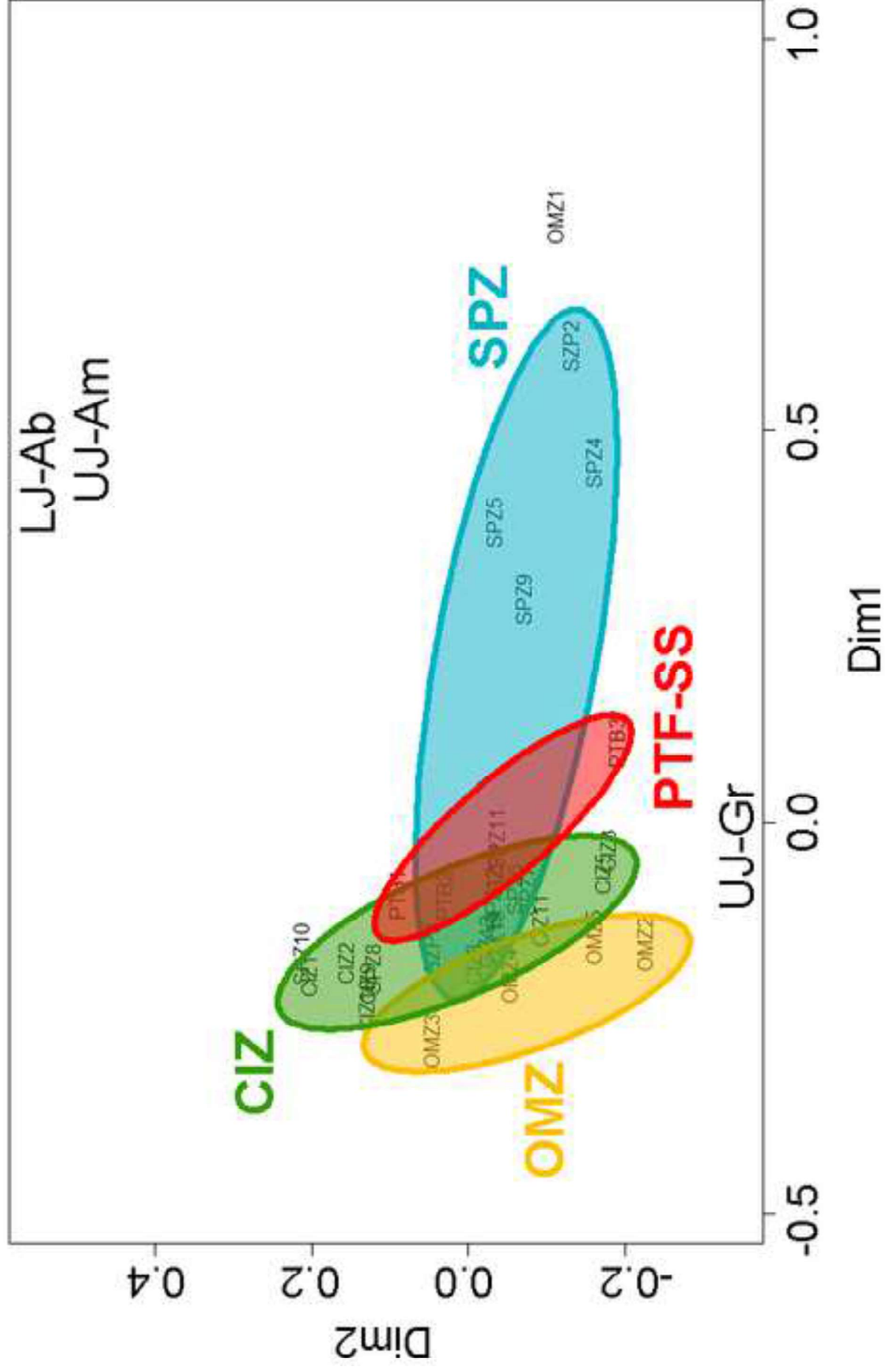
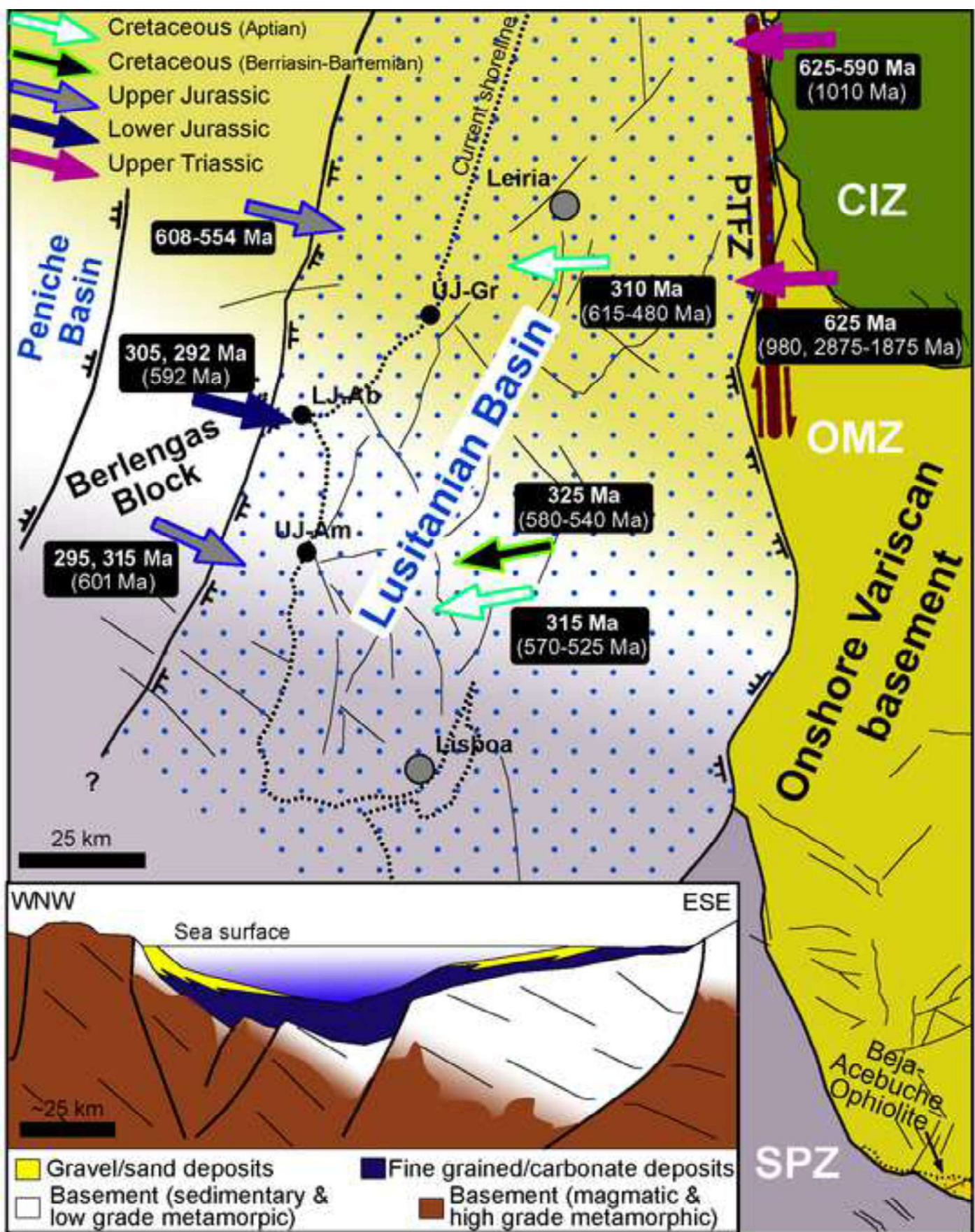


Figure 6

Figure 7

[Click here to access/download;Figure;Fig.7.jpg](#)





Click here to access/download
Supplementary Material
SupplementaryFile_Data.xlsx

